bioRxiv preprint doi: https://doi.org/10.1101/2020.07.02.185454; this version posted July 3, 2020. The copyright holder for this preprint (which was not certified by peer review) is the author/funder, who has granted bioRxiv a license to display the preprint in perpetuity. It is made available under aCC-BY-ND 4.0 International license.

An open-source experimental framework for automation of cell biology experiments

Pavel Katunin[1], Ashley Cadby[2] and Anton Nikolaev[3]*
[1]Fresco labs, London, UK and ITMO University, St. Petersburg, Russia
[2]Department of Physics and Astronomy, University of Sheffield, Sheffield, UK
[3]Department of Biological Sciences, University of Sheffield, Sheffield, UK
*address for correspondence: a.nikolaev@sheffield.ac.uk

Key points

-We present an open source framework for automation of cell biology experiments
-The framework consists of an XY platform, application of up to 8 solutions and a small epifluorescent microscope
-Very cheap (£300 without a fluorescent microscope and £2500 with a fluorescent microscope), customisable, 3D printable
-Can be used in a variety of biological applications such as imaging of fluorescent reporters, optimisation of treatment conditions and immuno-labelling

Abstract

Modern data analysis methods, such as deep learning, have been successfully applied to a number of biological and medical questions. For these methods to be efficient, a large number of high quality experiments need to be conducted, which requires a high degree of automation. Here we report an open-source hardware that allows for automatic high-throughput generation of large amounts of biological data. The hardware consists of an automatic XY-stage for moving multiwell plates containing growing cells; a perfusion manifold allowing application (perfusion) of up to 8 different solutions; and a small epifluorescent microscope. It is extremely cheap (£300 without and £2500 with a fluorescent microscope) and can be quickly customised for individual experimental needs.

Introduction

Deep learning and artificial neural networks (ANN) developed in the past decade have been proven useful for image analysis, optimisation tasks and robotics[1-3]. They are also becoming increasingly popular in solving biological problems. For example, ANN based algorithms of cell segmentation are more accurate and much faster than conventional methods[4]. Deep learning also helps to detect transformed cells in human tissues [5, 6], optimise treatment conditions [7] and explain animal behaviour[8]. Recently, an online platform has been developed to allow researchers without any prior knowledge of deep learning to use it in their own applications, further increasing the usefulness of deep learning as an analytical tool. [9].

One important consideration that has to be taken into account when applying deep learning and other machine learning methods is the size of the training datasets. Typically, deep learning requires thousands or tens of thousands of data points[10]. This is often not feasible in biological experiments as they often take a long time to conduct. Thus, there is a demand for automated

bioRxiv preprint doi: https://doi.org/10.1101/2020.07.02.185454; this version posted July 3, 2020. The copyright holder for this preprint (which was not certified by peer review) is the author/funder, who has granted bioRxiv a license to display the preprint in perpetuity. It is made available under aCC-BY-ND 4.0 International license.

systems that would allow hundreds or thousands of experiments to be performed simultaneously. Commercially available automation tools are useful, however these are expensive (>$10000-15000), large, non-flexible and mainly focus on solution handling. Importantly, experimental automation requires image analysis and application of solutions performed simultaneously, while many commercially available microscopes provide limited possibility for such closed loop experiments. Therefore, there is a demand for an open-source system that combines high-throughput microscopy in multiwell plates, automated solution application and simultaneous data analysis.

Here we developed an open-source experimental framework allowing for automated cell biology experiments. It is cheap, easily customisable and allows for up to 384 experiments to be performed simultaneously or sequentially. Its small epifluorescent microscope can be used to perform imaging of fluorescent reporters (e.g. GCaMP or synthetic calcium dyes, [11]) or fixed samples labelled with fluorescent antibodies. The proposed experimental framework will make generation of biological data quicker, more accurate and on a larger scale.

Results

Hardware description

1. Mechanical parts

The hardware (Fig.1A,B) consists of several principal modules: the X-Y stage (Fig.1C) moving a multiwell plate horizontally; a perfusion manifold performing application of 8 solutions into individual wells (Fig.2) and a small, autofocusing epifluorescent microscope (Fig.3). All files for 3D printing are available at https://github.com/frescolabs/FrescoM

The perfusion manifold (Fig.2) consists of a holder for 8 gel loading tips attached to flexible tubings via luer connectors. An additional 9th tip is connected to a peristaltic pump and a glass capillary. It is located higher than the application tips, thus providing constant solution height in each well. Solution change in individual wells is achieved by perfusing the wells with three to five well volumes. The perfusion manifold is connected to a vertically oriented linear actuator consisting of MGN12 rail, T8 lead screw and a Nema 17 motor, all attached to an arch fixed on the base parts. Standard syringe pumps are used for solution application. The 3D printed details and building instruction are provided in https://github.com/frescolabs/FrescoM

The schematics of the fluorescent microscope are shown in Fig3A. It is a standard inverted microscopy system with the following key features. We use non-infinity corrected objective (or, alternatively, small aspheric lens, f=2.75, NA=0.64), 100 mm camera lens (D=25.4 mm) and no tube lens. The GFP cube consists of blue and green Thorlabs filters (MF469-35 and MF525-39) and a dichroic mirror (MD498, Thorlabs). The objective is not attached to the rest of the microscope but is moving separately in a Z-stage (Fig. 3B). If the size of the sample is an issue, a more expensive infinity corrected objective can be used instead. In this case, there will be no fluctuations in the estimated size when focusing varies from well to well.

bioRxiv preprint doi: https://doi.org/10.1101/2020.07.02.185454; this version posted July 3, 2020. The copyright holder for this preprint (which was not certified by peer review) is the author/funder, who has granted bioRxiv a license to display the preprint in perpetuity. It is made available under aCC-BY-ND 4.0 International license.

A

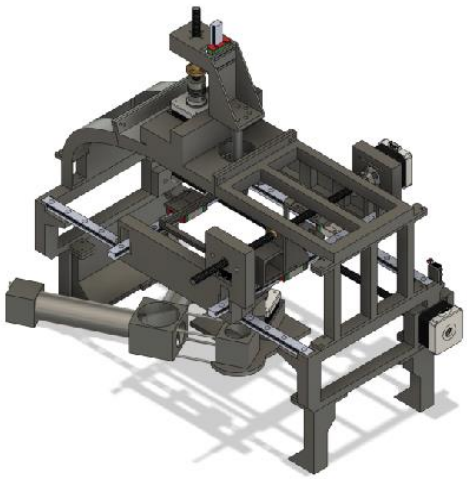

B

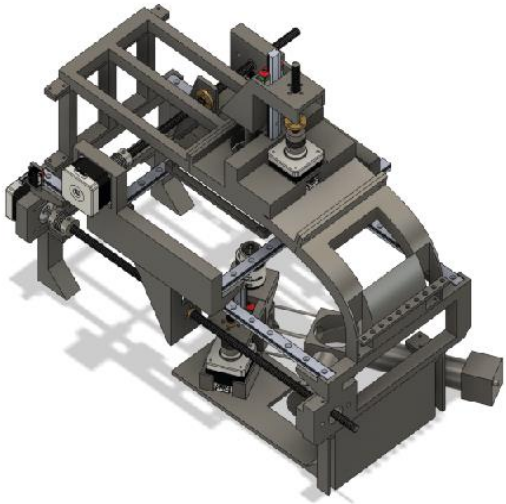

C

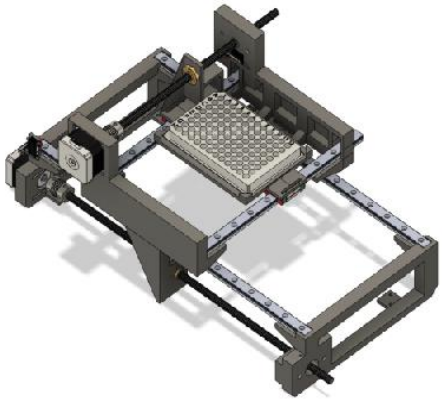

Fig.1 Overview of the hardware design. A, B- Entire hardware assembled and shown from two different points of view. The hardware consists of 3 modules: XY platform moving in horizontal directions; perfusion manifold moving up and down, epifluorescent microscope with a Z-stage.

The XY-stage (both bottom and top parts) consists of two vertical 3D printable details connected together by two horizontal linear motion rails (MGN12/MGN12H). Nema 17 motors are attached and connected to T8 screws. Rotation of the stepper motor moves the leading screw that is attached to either the top platform or to a plate holder. Movement can be as small as several tens of micrometers.

bioRxiv preprint doi: https://doi.org/10.1101/2020.07.02.185454; this version posted July 3, 2020. The copyright holder for this preprint (which was not certified by peer review) is the author/funder, who has granted bioRxiv a license to display the preprint in perpetuity. It is made available under aCC-BY-ND 4.0 International license.

2. Automatic control and electric circuit

All motors are operated via 3 CNC shields connected to Arduino Mega via a PCB board (Fig. 4A, Fig4B). Shield 1 operates the XY stage, perfusion module and autofocusing (Arduino pins 5-12 and enabling pin 13). Shields 2 and 3 operate 8 perfusion pumps (Arduino pins 23-53, odd numbers). In order for the software to have accurate estimates of the position of each axis and pump, endstops are attached to the rail of each axis (Arduino pins 22-44, even numbers).

Additional pins are reserved for microSD card (Arduino pins 46-52, even numbers), rotary encoder (Arduino pins 2-4) and small LCD display connected to Arduino via i2c protocol (Arduino pins A4, A5). The circuit can be modified to accommodate more CNC shields to increase the overall number of pumps to 22.

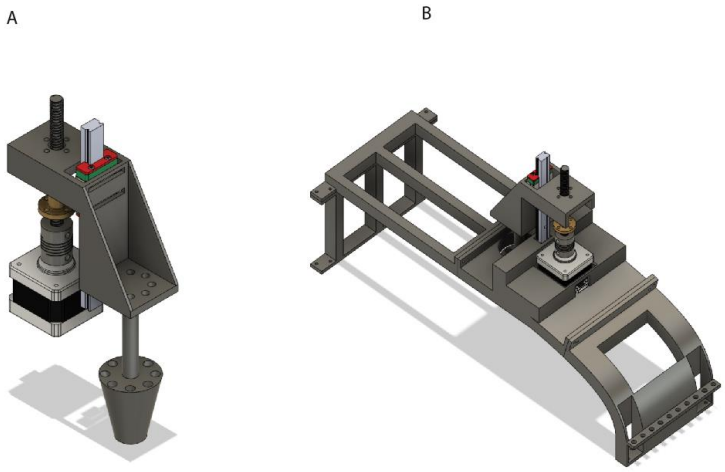

Fig.2 Perfusion system. A- perfusion manifold for 8 syringe pumps and one peristaltic pump for sucking the excess of liquid. Manifold holds 8 pipette tips and an additional one connected to the peristaltic pump. The latter is located slightly higher than others, which helps to keep the volume in each well constant. The manifold is fixed on a linear actuator and is driven by a Nema 17 motor. The whole system is fixed on an arch (B) located above the XY stage.

3. Assembly instructions

The entire solution application hardware consists of 14 3D printed parts, 6 linear rails, 4 Nema17 motors with adapters and 4 high precision T8 screws with a lead screw. Each pump consists of two 3D printed parts, one rod (8 mm), one linear bearing LM8UU, one T8 screw and a Nema 17 motor.

Assembling XY platform

1. 3D print all details
2. Assemble base platform by inserting 2 long linear rails into the base details
3. Insert Nema motor into the base and fix using M3 screws
4. Assemble top horizontal platform by inserting 2 shorter linear rails into the top details
5. Insert Nema motor into the top horizontal platform and fix using M3 screws
6. Insert lead screw into the top platform
7. Pass bottom high precision screw into the lead screw

bioRxiv preprint doi: https://doi.org/10.1101/2020.07.02.185454; this version posted July 3, 2020. The copyright holder for this preprint (which was not certified by peer review) is the author/funder, who has granted bioRxiv a license to display the preprint in perpetuity. It is made available under aCC-BY-ND 4.0 International license.

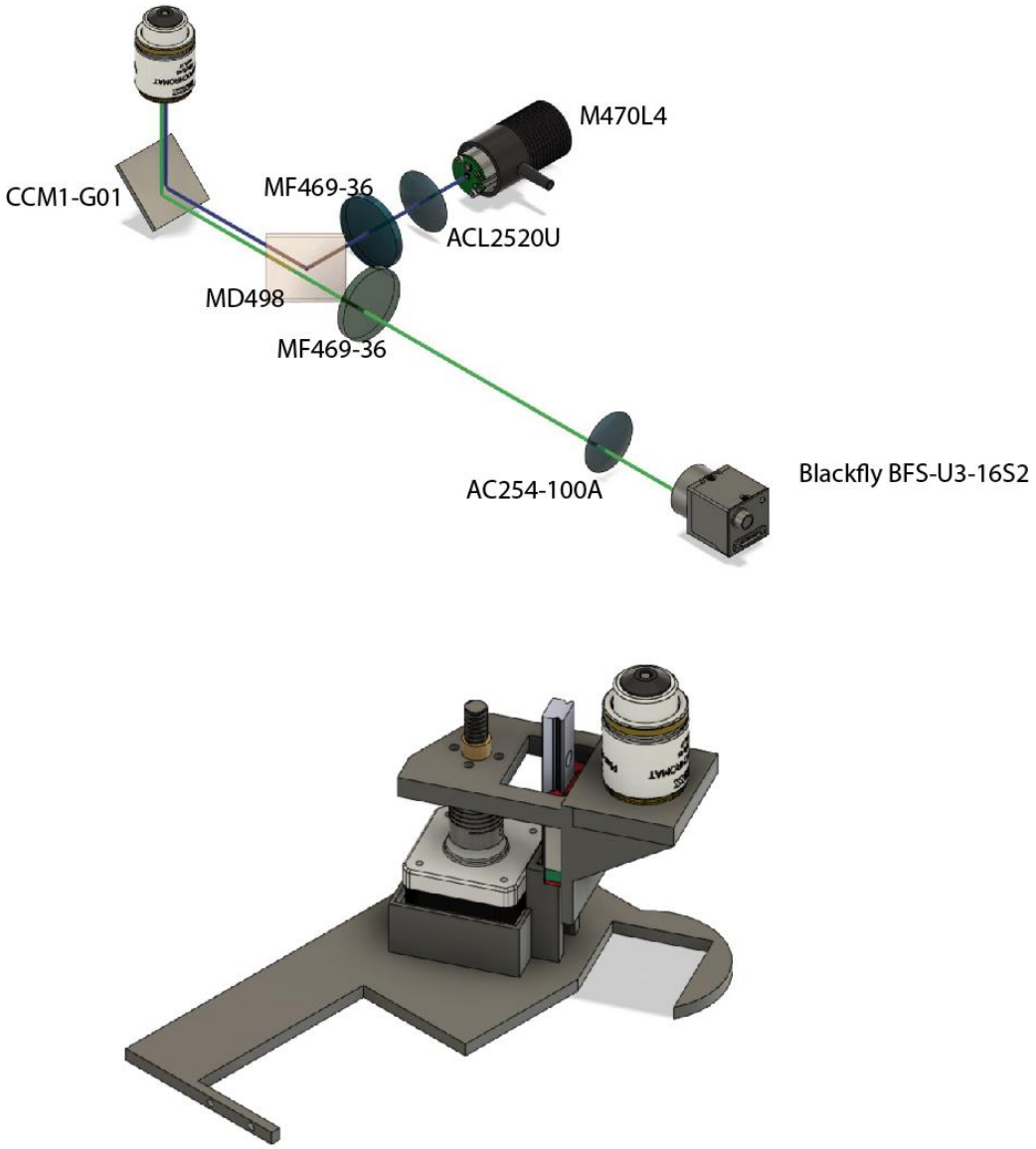

Fig.3. Mini fluorescent microscope schematic (A) and the autofocusing system (B). A- design of the optical part of the microscope. Numbers represent item numbers for each part. All parts except the camera are from Thorlabs, Inc. The system implements standard inverted fluorescent microscopy with the objective attached separately to a vertically oriented linear actuator driven by a Nema 17 motor.

bioRxiv preprint doi: https://doi.org/10.1101/2020.07.02.185454; this version posted July 3, 2020. The copyright holder for this preprint (which was not certified by peer review) is the author/funder, who has granted bioRxiv a license to display the preprint in perpetuity. It is made available under aCC-BY-ND 4.0 International license.

8. Put top XY part on top of bottom XY part, and connect high precision screw with Nema 17 motor using Insert 1 lead screw into the plate holder
9. Pass top high precision screw through the lead screw and connect to Nema 17 motor
10. Use 8 M3 screws to fix top platform on bottom platform and plate holder on the top platform

Assembling the perfusion manifold

1. Insert 8 pipette gel loading tips into the 3D printed manifold
2. Connect gel loading tips to flexible tubings using luer connectors
3. Attach an additional tip to the manifold side and connect it to a peristaltic pump. Cut the tip so that it is positioned 5-7 mm above the other tips
4. Connect 1 short linear rail into the manifold
5. Insert 1 lead screw into the manifold
6. Pass 1 short high precision screw into lead screw and connect to 1 Nema motor
7. Attach the entire system on two precision screws
8. Attach the other semi-arc and fix both halves with screws
9. Assemble all parts together on the XY platform

Assembling the Z-stage

1. Insert 1 Nema 17 motor into the base part
2. Insert one objective into the bottom part
3. Connect both parts with one precision screw and a small linear rail
4. Connect the Z stage to theXY platform

Assembling the mini microscope

The following instruction (Fig.4) describes how to assemble a small fluorescent microscope using Thorlabs details. The cost of the current configuration is £2000. This can be reduced by £450 if a cheaper LED and constant current driver is used. See https://github.com/Frescolabs/FrescoM for additional instructions.

1. Connect one mirror cube with two or 4 assemble rods
2. Connect filter cube
3. Insert 1 dichroic mirror into the filter cube as described in Thorlabs website
4. Insert excitation and emission filters into short SM1 tubes, fix with SM1RR retaining rings and connect the filter cube
5. Insert the 100mm focal distance lens to 100 mm SM1 tube and connect to the short emission filter SM1 tube.
6. Insert one 20 mm lens into a short SM1 tube and connect to the excitation filter to focus excitation light onto the sample
7. Connect mounted LED (e.g. M470L4)
8. Connect the mini-microscope to the Z-focusing system

bioRxiv preprint doi: https://doi.org/10.1101/2020.07.02.185454; this version posted July 3, 2020. The copyright holder for this preprint (which was not certified by peer review) is the author/funder, who has granted bioRxiv a license to display the preprint in perpetuity. It is made available under aCC-BY-ND 4.0 International license.

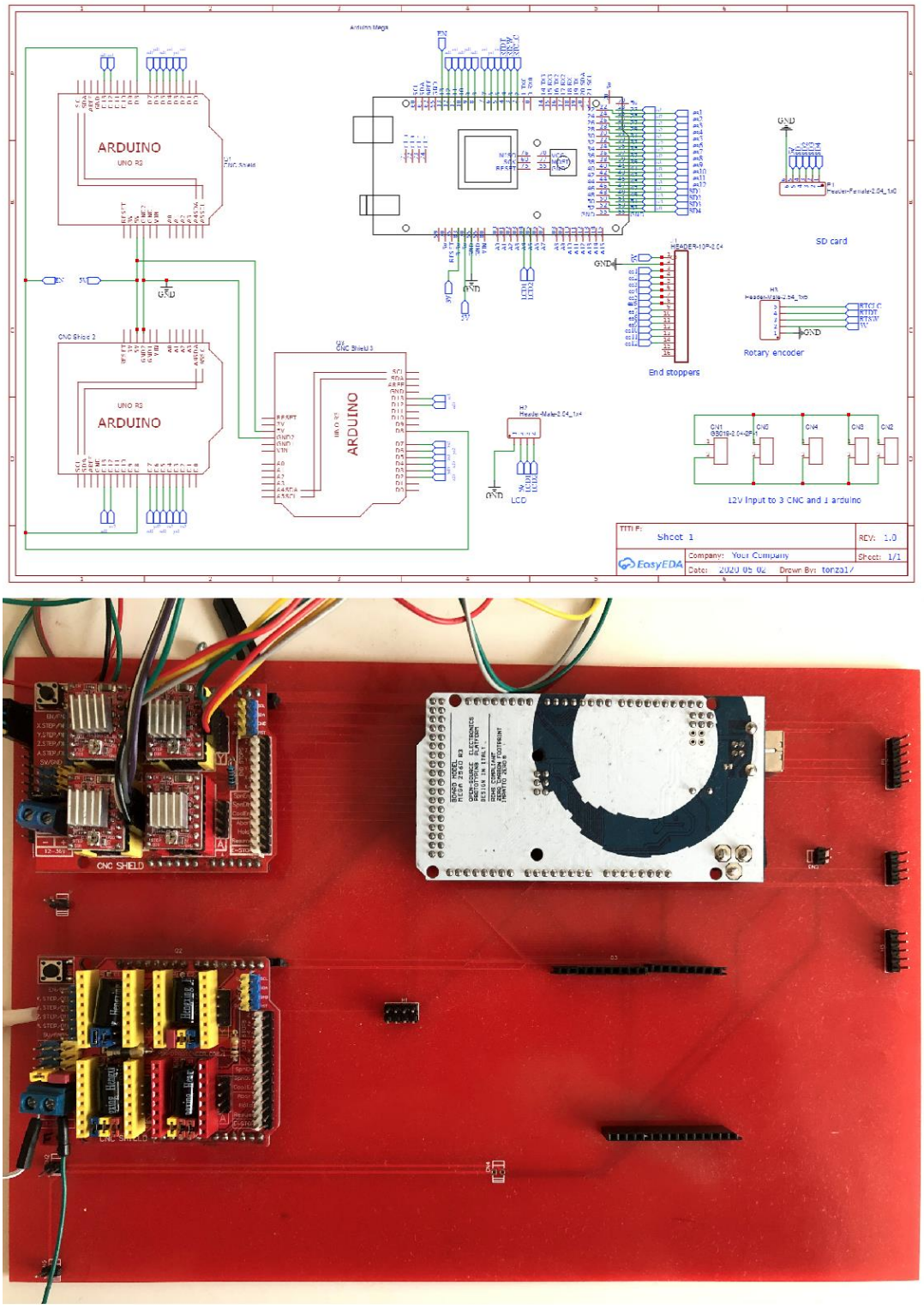

Fig.4 Electric circuits and PCB board controlling the main hardware.
A - schematics of the electric circuit. The main circuit consists of slots for three CNC Shields, Arduino Mega and 12 inputs for end switches. B- The resulting circuit board with one CNC shield removed. Two CNC shields are shown in red. Arduino Mega is shown in white.

bioRxiv preprint doi: https://doi.org/10.1101/2020.07.02.185454; this version posted July 3, 2020. The copyright holder for this preprint (which was not certified by peer review) is the author/funder, who has granted bioRxiv a license to display the preprint in perpetuity. It is made available under aCC-BY-ND 4.0 International license.

4. Software

4.1. Firmware

The hardware is operated via an Arduino board that receives instructions from a computer via serial port. Functionality where commands are sent via wifi module or stored in a file in a microSD card are reserved for future versions (Fig.4A). The commands shown in Table 1.

Command	Action
Z	X,Y, Z go to zero
S [motor number], e.g. S 001	Motor 1 stops running
P [motor number] [steps], e.g. P 000 1000	Motor 0 moves 1000 steps
M [motor number] e.g. M 002	Motor 2 moves until command stop is received
X [motor number], e.g X 000	Return motor's position via serial port
L [value]	Microscope's excitatory LED switch on (value =1) LED switch off (value = 0)

Table 1. List of commands used by Arduino to operate the main hardware. The Arduino code can be downloaded from https://github.com/frescolabs/FrescoM/blob/master/firmware

4.2. Python software

The main operating software is written in Python 3 and can be downloaded from https://github.com/frescolabs/FrescoM/blob/master/software
Detailed instructions can also be downloaded from https://github.com/frescolabs/FrescoM/blob/master/software

The software is very basic, easy to use and modifiable to fit individual needs. The key functions are as follows:

1. Start live fluorescent imaging without recording.
2. Move platform forward, backward, left and right.
3. Move the application manifold up and down.
4. Return to zero position -- returns XY platform and the application manifold into the start position.
5. Set top-right and set bottom-right positions of the multiwell plate.
6. Move pump - moves pumps forwards and backwards. To be used to fill pumps with solutions and cleaning the system after the experiment.
7. Start experiment. Runs experiment from a list of commands saved in a file. The file should contain four columns: time, well number, pump number, number of steps. The later number sets up the volume needed for application and represents the number of steps that motor should move.

bioRxiv preprint doi: https://doi.org/10.1101/2020.07.02.185454; this version posted July 3, 2020. The copyright holder for this preprint (which was not certified by peer review) is the author/funder, who has granted bioRxiv a license to display the preprint in perpetuity. It is made available under aCC-BY-ND 4.0 International license.

5. Performance

5.1 Calcium imaging using fluorescent mini microscopes

To test how well fluorescent mini-microscopes perform we labelled HCT-116 cells with synthetic calcium dye (Oregon Green) and imaged calcium dynamics in response to 100 μM ATP. Fig.5 A, B shows representative experiment. The quality of the resulting images was sufficient to identify individual cells (particularly in less confluent areas) and calcium response in individual cells can be defined.

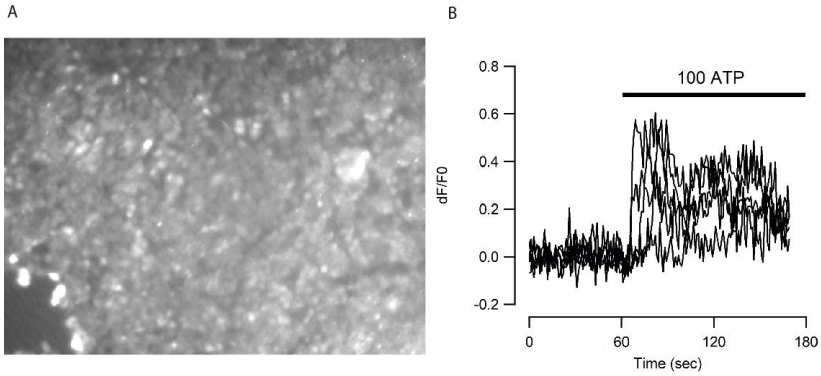

Fig.5 Performance of the microscope. A, B - calcium imaging of HCT116 cells. Cells were labelled for 30 min with 1 μM Oregon Green and imaged with sampling frequency 1 frame per second. A- HCT116 cells imaged using 2.75 objective lens(C392TME-A, Thorlabs). Average of 70 frames. Scale bar not shown. B- 5 examples of calcium dynamics in HCT116 cells in response to application of 100 μM ATP from the same experiment.

Discussion

There is a high demand for designing affordable and flexible tools for high-scale generation of biological data. Here we report a combination of hardware and software that allows for up to several hundred cell biology experiments performed simultaneously and automatically. Below we discuss applicability of the developed platform and future improvements.

Importance of automation of biological experiments

Automation of biological experiments is important for two main reasons. First, a large number of data points are required when using modern methods of analysis, such as machine learning and deep learning. A good convolutional neural network algorithm typically requires in the region of 10,000 to 100,000 data points [10]. Considering that there are only a few thousands of cells in a field of view, the same experiments need to be reproduced 10 to 100 times. This number increases significantly if the experimental goal is to optimise conditions for biological experiments.

Second, there is a growing discussion on reproducibility of biological data [12-15].This is particularly crucial when the results have direct translational applications and can affect future expensive clinical trials. The reproducibility can be improved when the experiments are standardised and when experimentation and data analysis are performed automatically to avoid human errors. The reproducibility of experiments can be further improved when performed on different sources (different cell types, cells with different genetic backgrounds, etc.) further highlighting the necessity of automation of biological experiments.

bioRxiv preprint doi: https://doi.org/10.1101/2020.07.02.185454; this version posted July 3, 2020. The copyright holder for this preprint (which was not certified by peer review) is the author/funder, who has granted bioRxiv a license to display the preprint in perpetuity. It is made available under aCC-BY-ND 4.0 International license.

Applicability

1. High-throughput screening experiments

Expansion of the compound libraries [16-18] provided a valuable tool to search for new chemicals affecting biological functions. For example, drugs affecting physiological signalling pathways (e.g. GPCRs, etc.) can be assessed by calcium imaging [19-21] or any other forms of functional imaging with a single cell resolution. However, this requires a large number of experiments which is laborious. The framework developed here, easily allows for automatic labelling of cells with a calcium dye, application of different agonists and measurements of calcium signalling (Fig.5) in a large number of wells.

2. Optimisation experiments

Many biological experiments require optimization of treatment conditions. For example, differentiation of stem cells requires treatment with a large number of growth factors and morphogens at different times and with different dynamics [22, 23]. The framework developed here, allows for experiments such as this be performed in an automatic manner. The outcome of an experiment can then be automatically tested using one of two methods: immunolabeling of cells with antibodies against appropriate surface markers or a functional experiment (e.g. neurons can be detected by calcium imaging and application of potassium chloride or neurotransmitters).

3. Large scale characterisation of cells derived from individual patients

Substitution of standard cell lines with cells recently derived from individual patients is now becoming increasingly important[24, 25]. The experimental framework developed here would allow a large number of cell lines derived from individual experiments to be tested in a standardized way.

4. Routine cell biology procedures

The developed experimental platform will also be useful in routine lab procedures such as concentration dependence curves, cell dilutions, cytotoxicity studies and others.

Further improvements

The modular structure of the platform developed here allows for fairly easy future adjustments to fit individual experimental needs. For example,

1. Substitution of the microscope (Fig.1) with a heat-block will allow to incorporate PCR capability into the analysis. Other means of detection of the experimental outcome (e.g. mini spectrophotometer) will increase the amount experiments that can be performed.
2. Currently, the microscope only provides simple wide-field one colour fluorescence. It can be improved by adding some optical sectioning functionality such as HiLo or light sheet microscopy [26]f. The price of the microscope can also be significantly reduced if a custom built LED system is used alongside filter cubes from old fluorescent microscopes. This will reduce the price by £250 and £450 respectively.
3. The number of applied solutions can be increased by redesigning the solution application manifold.

bioRxiv preprint doi: https://doi.org/10.1101/2020.07.02.185454; this version posted July 3, 2020. The copyright holder for this preprint (which was not certified by peer review) is the author/funder, who has granted bioRxiv a license to display the preprint in perpetuity. It is made available under aCC-BY-ND 4.0 International license.

4. Cleaning the multi-syringe system can be automated by adding storages for distilled water, alcohol and waste.
5. Experiments can take a long time to perform and cells may need occasional passaging. An algorithm of detecting confluence and then splitting cells into new wells would allow the outcome of experiments to not be influenced by the overconfluence. In addition to that, selection of individual cells and transferring them into a new well will allow for generation selection of new clones for generation of new lines using transfection or CRISPR.

Acknowledgements

Microscopes were designed and built by AN and AC and supported by the University of Sheffield Alumni Fund. The mechanics and electronics was designed and implemented by PK and AN. We thank Elliot Birkett for reading and comments on the manuscript.

References

1. Hinton, B., Ma, L., Mahmoudzadeh, A.P., Malkov, S., Fan, B., Greenwood, H., Joe, B., Lee, V., Kerlikowske, K., and Shepherd, J. (2019). Deep learning networks find unique mammographic differences in previous negative mammograms between interval and screen-detected cancers: a case-case study. Cancer Imaging *19*, 41.
2. Hinton, G. (2018). Deep Learning-A Technology With the Potential to Transform Health Care. JAMA *320*, 1101-1102.
3. LeCun, Y., Bengio, Y., and Hinton, G. (2015). Deep learning. Nature *521*, 436-444.
4. Hilsenbeck, O., Schwarzfischer, M., Loeffler, D., Dimopoulos, S., Hastreiter, S., Marr, C., Theis, F.J., and Schroeder, T. (2017). fastER: a user-friendly tool for ultrafast and robust cell segmentation in large-scale microscopy. Bioinformatics *33*, 2020-2028.
5. Coudray, N., Ocampo, P.S., Sakellaropoulos, T., Narula, N., Snuderl, M., Fenyo, D., Moreira, A.L., Razavian, N., and Tsirigos, A. (2018). Classification and mutation prediction from non-small cell lung cancer histopathology images using deep learning. Nat Med *24*, 1559-1567.
6. Van Valen, D.A., Kudo, T., Lane, K.M., Macklin, D.N., Quach, N.T., DeFelice, M.M., Maayan, I., Tanouchi, Y., Ashley, E.A., and Covert, M.W. (2016). Deep Learning Automates the Quantitative Analysis of Individual Cells in Live-Cell Imaging Experiments. PLoS Comput Biol *12*, e1005177.
7. Kusumoto, D., and Yuasa, S. (2019). The application of convolutional neural network to stem cell biology. Inflamm Regen *39*, 14.
8. Heras, F.J.H., Romero-Ferrero, F., Hinz, R.C., and de Polavieja, G.G. (2019). Deep attention networks reveal the rules of collective motion in zebrafish. PLoS Comput Biol *15*, e1007354.
9. https://www.biorxiv.org/content/10.1101/2020.03.20.000133v1.
10. Mahoney Deep Learning vs. Traditional Computer Vision. https://arxiv.org/ftp/arxiv/papers/1910/1910.13796.pdf.
11. Razlivanov, I., Liew, T., Moore, E.W., Al-Kathiri, A., Bartram, T., Kuvshinov, D., and Nikolaev, A. (2018). Long-term imaging of calcium dynamics using genetically encoded calcium indicators and automatic tracking of cultured cells. Biotechniques *65*, 37-39.
12. Freedman, L.P., Cockburn, I.M., and Simcoe, T.S. (2015). The Economics of Reproducibility in Preclinical Research. PLoS Biol *13*, e1002165.
13. Ioannidis, J.P. (2005). Why most published research findings are false. PLoS Med *2*, e124.

bioRxiv preprint doi: https://doi.org/10.1101/2020.07.02.185454; this version posted July 3, 2020. The copyright holder for this preprint (which was not certified by peer review) is the author/funder, who has granted bioRxiv a license to display the preprint in perpetuity. It is made available under aCC-BY-ND 4.0 International license.

14. Ioannidis, J.P. (2007). Why most published research findings are false: author's reply to Goodman and Greenland. PLoS Med *4*, e215.
15. Ioannidis, J.P. (2014). How to make more published research true. PLoS Med *11*, e1001747.
16. Cases, M., Garcia-Serna, R., Hettne, K., Weeber, M., van der Lei, J., Boyer, S., and Mestres, J. (2005). Chemical and biological profiling of an annotated compound library directed to the nuclear receptor family. Curr Top Med Chem *5*, 763-772.
17. Rickardson, L., Fryknas, M., Haglund, C., Lovborg, H., Nygren, P., Gustafsson, M.G., Isaksson, A., and Larsson, R. (2006). Screening of an annotated compound library for drug activity in a resistant myeloma cell line. Cancer Chemother Pharmacol *58*, 749-758.
18. Root, D.E., Flaherty, S.P., Kelley, B.P., and Stockwell, B.R. (2003). Biological mechanism profiling using an annotated compound library. Chem Biol *10*, 881-892.
19. Berridge, M.J. (2001). The versatility and complexity of calcium signalling. Novartis Found Symp *239*, 52-64; discussion 64-57, 150-159.
20. Berridge, M.J., Bootman, M.D., and Roderick, H.L. (2003). Calcium signalling: dynamics, homeostasis and remodelling. Nat Rev Mol Cell Biol *4*, 517-529.
21. Bootman, M.D., Berridge, M.J., and Roderick, H.L. (2002). Calcium signalling: more messengers, more channels, more complexity. Curr Biol *12*, R563-565.
22. Kim, J.H., Auerbach, J.M., Rodriguez-Gomez, J.A., Velasco, I., Gavin, D., Lumelsky, N., Lee, S.H., Nguyen, J., Sanchez-Pernaute, R., Bankiewicz, K., et al. (2002). Dopamine neurons derived from embryonic stem cells function in an animal model of Parkinson's disease. Nature *418*, 50-56.
23. Panchision, D.M., and McKay, R.D. (2002). The control of neural stem cells by morphogenic signals. Curr Opin Genet Dev *12*, 478-487.
24. Rominiyi, O., Al-Tamimi, Y., and Collis, S.J. (2019). The 'Ins and Outs' of Early Preclinical Models for Brain Tumor Research: Are They Valuable and Have We Been Doing It Wrong? Cancers (Basel) *11*.
25. Stringer, B.W., Day, B.W., D'Souza, R.C.J., Jamieson, P.R., Ensbey, K.S., Bruce, Z.C., Lim, Y.C., Goasdoue, K., Offenhauser, C., Akgul, S., et al. (2019). A reference collection of patient-derived cell line and xenograft models of proneural, classical and mesenchymal glioblastoma. Sci Rep *9*, 4902.
26. https://www.microscopyu.com/techniques/light-sheet/light-sheet-fluorescence-microscopy.